Proceedings, Bicycle and Motorcycle Dynamics 2019
Symposium on the Dynamics and Control of Single Track Vehicles,
9 – 11 September 2019, University of Padova, Italy

Study of Personal Mobility Vehicle (PMV) with active inward tilting mechanism on obstacle avoidance and on energy efficiency

T. Haraguchi[*], I. Kageyama[#], T. Kaneko[†]

[*] Institutes of Innovation for Future Society
Nagoya University
Furo-cho, Chikusa-ku, Nagoya 464-8603, Japan
e-mail: haraguchi@nagoya-u.jp

[#] College of Industrial Technology
Nihon University
1-2-1 Izumi-cho, Narashino, 275-8575 Japan
e-mail: kageyama.ichiro@nihon-u.ac.jp

[†] Department of Mechanical Engineering for Transportation
Osaka Sangyo University
3-1-1 Nakagaito, Daito, 574-8530 Japan
e-mail: kaneko@tm.osaka-sandai.ac.jp

ABSTRACT

Traffic congestions and lack of parking spaces in urban areas, etc. may impair original benefits of cars, and now new ultra-small mobility concepts called Personal Mobility Vehicles (PMVs) are payed attention. Among them, PMVs with inward tilting mechanism in order to avoid overturning on turning as same as motorcycles look realistic in innovative new traffic systems. In this report, PMVs with active inward tilting mechanism with three wheels; double front wheels + single rear wheel and front steering + rear traction, are studied on front inner wheel lifting phenomena, on capability of obstacle avoidance and on energy balance of active tilting mechanism. Then, sufficient social acceptability of inward tilting type PMVs was shown.

Keywords: PMV, Active tilting, Inner wheel lifting, Obstacle avoidance, Energy efficiency.

1 INTRODUCTION

Although automobiles have improved life quality of human being, too much increase of vehicles number in use has potential to spoil original benefits of automobiles. Those are such as traffic congestion and lack of parking space in urban areas. From this reason, new ultra-small mobility concepts called personal mobility vehicles (PMVs) are now attracting attention [1][2].

PMVs with narrow total width are likely to be inward tilting type as same as motorcycles in order to avoid overturning on turning. Among them, tricycles with two front wheels and one rear wheel seems to be a good idea because of simplicity of vehicle configuration and security against overturning during braking as shown in Figure 1. General understanding of advantages and disadvantages on types of PMV is shown in Table 1.

Following concerns should be kept in mind as new PMV concepts with inward tilting mechanism.

Concerning point of PMVs with passive tilting mechanism
- Self-standing ability from stop to very low speed

Major concerns of PMVs with active tilting mechanism
- Inner wheel lifting on sudden steering input
- Capability on obstacle avoidance
- Energy consumption on active tilting system

Table 1. Advantage (✓) / Disadvantage (▼) on types of PMV

	Simple construction	Slow speed	Stability on braking	Obstacle avoidance
Single front wheel + Double rear wheels Front steering + Rear traction	✓		▼ Unstable	▼ U.S.
Double front wheels + Single rear wheel			✓	
Front steering + Rear traction				
Passive tilt mechanism	✓	▼ Falling		▼ Delay
Active tilt mechanism	▼ Active	✓		✓
Front traction + Rear steering	▼ Steer-by-wire			▼ Delay
Double front wheels + Double rear wheels	▼ 4 wheels		✓	
Front steering + Rear traction				
Passive tilt mechanism	✓	▼ Falling		▼ Delay
Active tilt mechanism	▼ Active	✓		✓

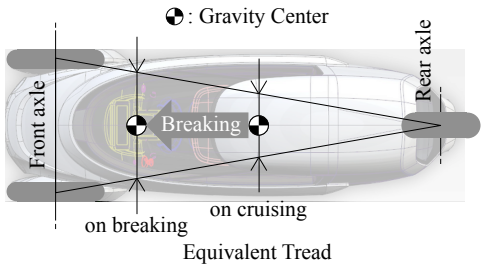

Figure 1. Equivalent tread is wider on breaking

1.1 Self-standing ability from stop to very low speed

In order to achieve both passive tilting mechanism and self-standing ability from stop to very low speed, it should be mechanical and simple mechanism. Although details are omitted this time, we devised self-standing mechanism and confirmed effectiveness of that mechanism using a motorcycle with two front wheels as shown in Figure 2.

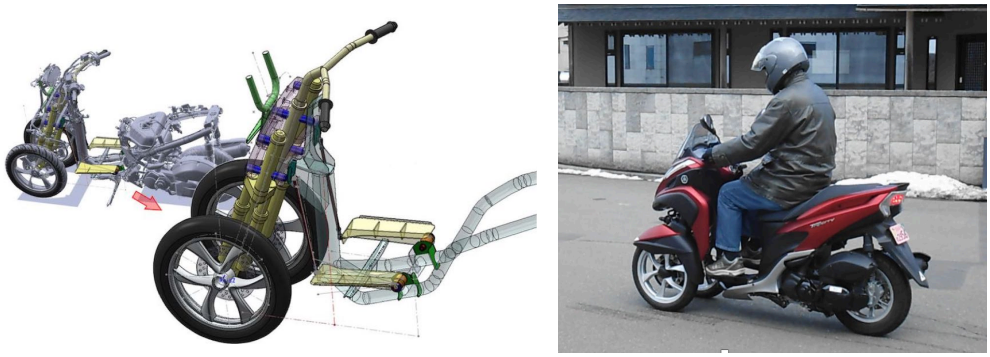

Figure 2. Self-standing mechanism was devised

1.2 Study of PMVs with active tilting mechanism

In this report, using multibody dynamics models described in next chapter, we study three concerns of PMVs with active tilting mechanism, and discuss social acceptability of inward tilting type PMVs.

2 MULTIBODY DYNAMICS MODEL

2.1 Vehicle model

Specifications of PMV are shown in Figure 3 and Table 2. Although overall length and width

are about 1/2 of passenger car, overall height is similar as passenger car. Therefore, inward tilting is necessary.

As a vehicle dynamics simulation tool, we used CarMaker from IPG Automotive in Germany. In order to construct tilting model with car simulation tool, following measures were taken.

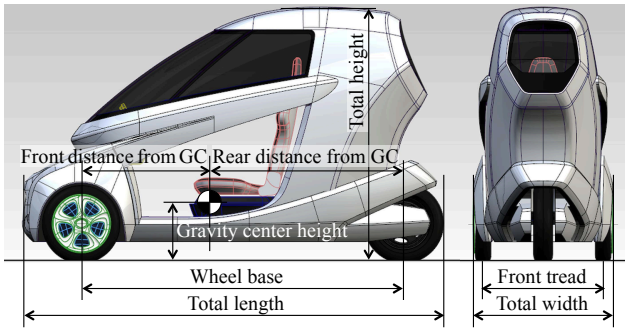

Figure 3. Dimensions of model vehicle

Table 2. Specifications of model vehicle

item	unit	value	item	unit	value
Total length	m	2.645	Total mass	kg	369.79
Total width	m	0.88	Front mass distribution	kg	222.057
Total height	m	1.445	Rear mass distribution	kg	147.733
Wheel base	m	2.02	Roll inertia moment	kgm^2	58.776
Front distance from GC	m	0.807	(Sprung inertia moment)	kgm^2	42.996
Rear distance from GC	m	1.213	Pitch inertia moment	kgm^2	197.328
Front tread	m	0.85	(Sprung inertia moment)	kgm^2	118
Gravity center height	m	0.358	Yaw inertia moment	kgm^2	187.280
Steering Gear Ratio	−	16.0	(Sprung inertia moment)	kgm^2	102.28

2.1.1 Suspension

As shown in Figure 4, forced torsional torque is applied to stabilizer bar. In this method, vehicle generates internal torque. Although mechanism might be different from PMVs having direct suspension stroke control mechanism, motion characteristics and external forces acting on this vehicle are same.

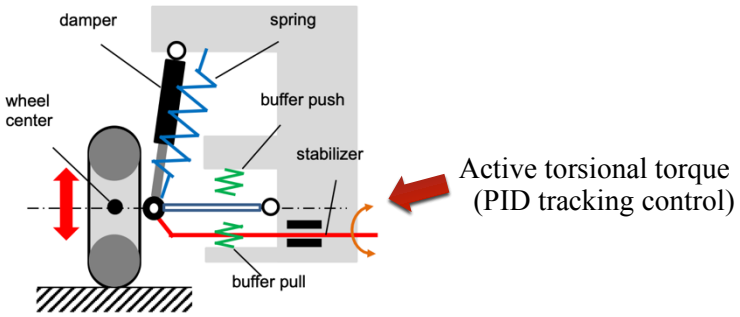

Figure 4. Torsional torque is applied to stabilizer bar

2.1.2 Target roll angle

Target tilting (roll) angle is given as shown in Equation (1), to balance against virtual lateral acceleration which is simply calculated from tire steered angles, wheel base and vehicle speed. Torsion torque of active stabilizer to get target roll angle is given by general PID tracking control. Initial values of control gain are shown in Equation (2).

$$TRA = A \tan^{-1}\left(\frac{\sin(\delta)\, v^2}{lg}\right) \quad \cdots \quad (1)$$

TRA ; Target Roll Angle
A ; User Amplification Factor
δ ; Tire Steered Angle

$$P = 4000\ ,\quad I = 100\ ,\quad D = 0 \qquad \cdots \quad (2)$$

v ; Vehicle Speed
l ; Wheel Base

2.1.3 Tire

PMVs with tilting mechanism are strongly influenced by tire camber characteristics. Therefore, we used a motorcycle tire model in CarMaker as shown in Figure 5 to consider side force on tire camber angle.

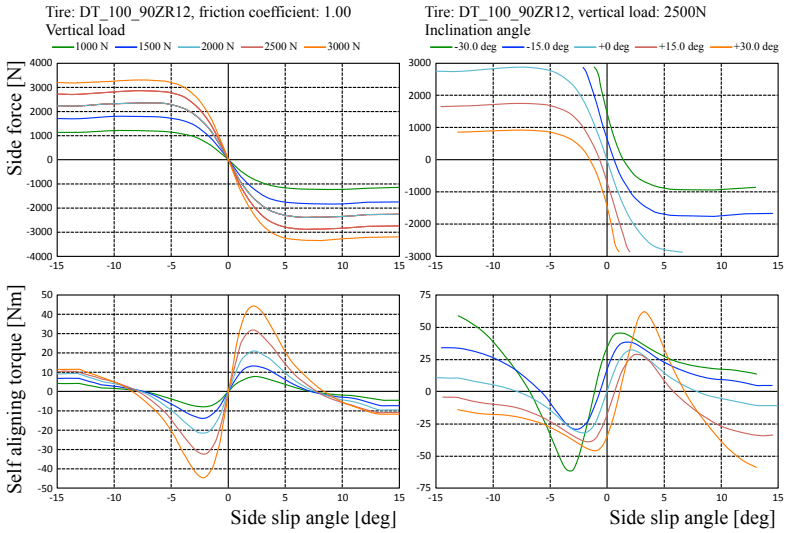

Figure 5. Motorcycle tire model is used in CarMaker

2.2 Driver model

IPGDriver from IPG Automotive attached to CarMaker is used as driver model on this study. IPGDriver understands vehicle characteristics and controls vehicle speed and steering wheel angle to trace given course based on forward quadratic prediction model.

3 INNER WHEEL LIFTING PHENOMENA

Active tilting mechanism forcibly applies strokes to suspension. In case roll response of sprung body is delayed, difference of vertical loads on front two wheels occurs. In worse cases, we face to inner wheel lifting phenomena [3][4]. Although lifting itself is not problem, divergent phenomena causes overturning. Therefore, repeated liftings are better to be avoided.

3.1 Understanding mechanism of lifting phenomena

Mechanism of front inner wheel lifting caused by sudden steering inputs is seemed to be as follows.

1) Inward roll response to steering input cannot be in time due to roll inertia moment.
2) Transitional front wheel slip angle due to vehicle response delay caused by yawing inertia moment, causes outward roll moment. This roll moment further delays inward roll response.
3) Too much rebound stroke of front outer wheel caused by inward roll response delay, lifts up front body. Pitching inertia moment delays recovery from front body lifting.

3.1.1 Influence of PID factors on roll angle tracking control

In order to study influence of three axes inertia moments to front inner wheel lifting phenomena during sudden steering inputs, it is inconvenient if vehicle has unstable roll phenomena (for example, roll vibration) without intentional steering input. As shown in Figure 6, when sprung roll

inertia moment (*Ixx**) is increased, vehicle becomes unstable in roll direction. Roll vibration starts with doubled *Ixx** even on straight running ahead. Overturning occurs with quadrupled *Ixx** without ability to continue straight running as shown in Figure 7.

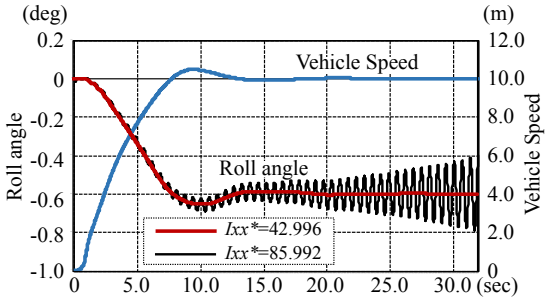

Figure 6. Unstable roll vibration with high *Ixx**

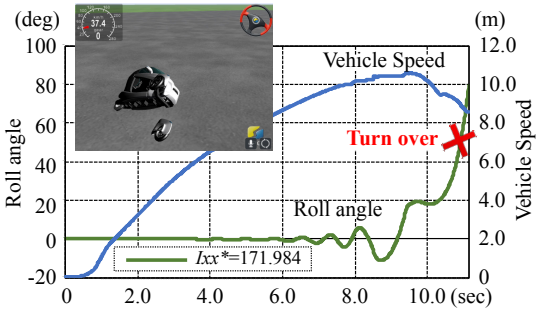

Figure 7. Turning over with too high *Ixx**

As shown in Figure 8, in case I gain was reduced by half (100 → 50), it was confirmed that roll vibration is suppressed even under previous condition (doubled *Ixx** and quadrupled *Ixx**) was confirmed. There is no roll vibration even roll inertia moment is quadrupled. We proceeded with I gain = 50 in order to eliminate disturbing effect of roll tracking control.

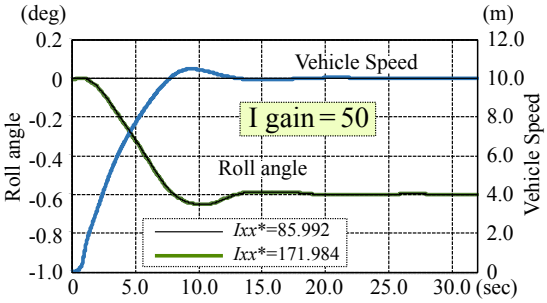

Figure 8. No roll vibration phenomena are observed (I = 100 → 50)

3.1.2 Steering input condition

Lateral displacement of motorcycles in severe obstacle avoidance scene is about 2 m. Steering input angle was set as initial condition to get this lateral displacement. Lateral displacement *LD* is proportional to steering angle *MA* and square of vehicle speed *v*, and inversely proportional to square of steering input frequency *f*, as in Equation (3).

$$LD \propto \frac{MA\, v^2}{f^2} \quad \cdots (3)$$

LD ; Lateral displacement
MA ; Steering wheel angle
v ; Vehicle Velocity
f ; Steering input frequency

Sinusoidal input of about 0.5 Hz ± 60 deg gives about 2 m lateral displacement *LD* at vehicle speed of 36 km/h (10 m/sec). Input frequency of 0.5 Hz is equivalent to quick lane change (L/C) operation of standard drivers on public roads.

3.1.3 Relation between steering angle and input frequency

Lateral displacement *LD* is expressed by Equation (3). Steering input angle *MA* proportioned to square of steering input frequency *f* gives maintained *LD* as shown in Figure 9. However, extreme increase of steering input angle *MA* means fairly severe condition for inner wheel lifting phenomena. Therefore, increasing steering input frequency *f* results in a sudden turnover.

Only steering input frequency *f* was changed while maintaining steering input angle *MA* = ± 60 deg without maintaining *LD* as shown in Figure 10. Minimum residual load of front left wheel

(inner wheel) is almost zero at $f = 0.71$ Hz, and inner wheel lifts clearly at $f = 1.0$ Hz. It can be understood that front inner wheel lifting is caused not only by large steering angle input but also directly by quick steering input.

Quick and large steering input is actually very difficult for human drivers. Effects of three axis inertia moments on front inner wheel lifting phenomena by sudden steering input were examined with 0.5 Hz (quick L/C) as upper limit of standard drivers' ability.

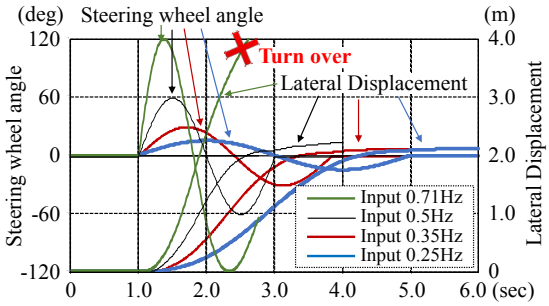

Figure 9. Steering angle proportioned to square of frequency results in sudden turnover (I = 50)

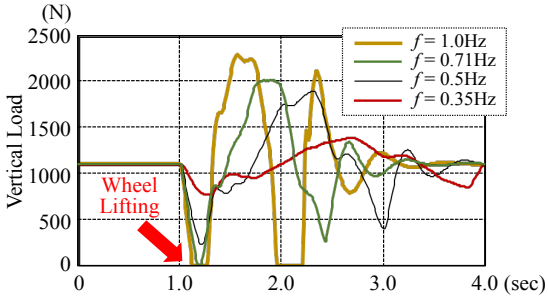

Figure 10. Quick steering input directly causes wheel lifting (I = 50)

3.1.4 Vehicle speed

Steering input angle *MA* inversely proportioned to square of vehicle speed *v* gives maintained *LD* as shown in Figure 11. However, in order to avoid obstacles actually, steering input frequency *f* needs to be increased in proportion to increase of vehicle speed *v*. Totally saying, *MA* is not decreased proportionally to square of vehicle speed *v* on actual obstacle avoidance as shown in Figure 12. Effects of three axis inertia moments on front inner wheel lifting phenomena by sudden steering input were examined with 36 km/h (10 m/sec).

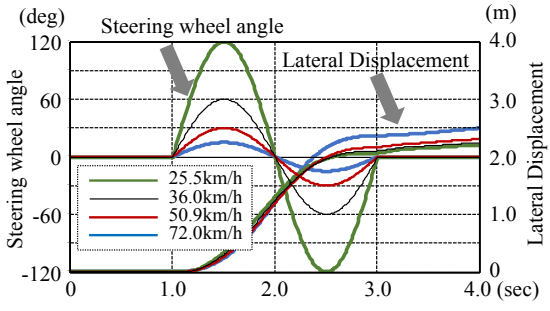

Figure 11. Required steering input angle (I = 50)

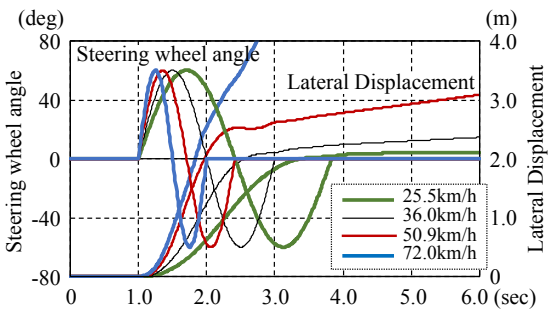

Figure 12. Influence of vehicle speed (I = 50)

3.2 Influences of three axis inertia moments

The effects of sprung inertia moments around three axes *Ixx**, *Iyy** and *Izz** were examined.

3.2.1 Influence of roll inertia moment

Influence of roll inertia moment was examined by parameterizing sprung roll inertia moment *Ixx**, out of whole vehicle roll inertia moment *Ixx* = 58.776 kgm^2. Figure 13 (I = 50, *f* = 0.5Hz) shows vehicle behavior at vehicle speed *v* = 36 km/h (10 m/sec), steering input frequency *f* = 0.5 Hz, sinusoidal steering angle *MA* = ± 60 deg, and roll tracking gain I = 50.

Larger *Ixx** clearly increase front inner wheel lifting. Although we do not face to phenomena when *Ixx** = 42.996 kgm^2 (standard), we face to almost zero vertical lord of inner wheel when twice *Ixx** = 85.992 kgm^2, and we face clearly to inner wheel lifting phenomenon when 4 times *Ixx** = 171.984 kgm^2.

Effect of roll inertia moment *Ixx** on sprung was confirmed also at *f* = 1.0 Hz (sudden L/C). As shown in Figure 13 (I = 50, *f* = 1.0 Hz), front inner wheel lifting occurs even when *Ixx** = 42.996 kgm^2 (standard).

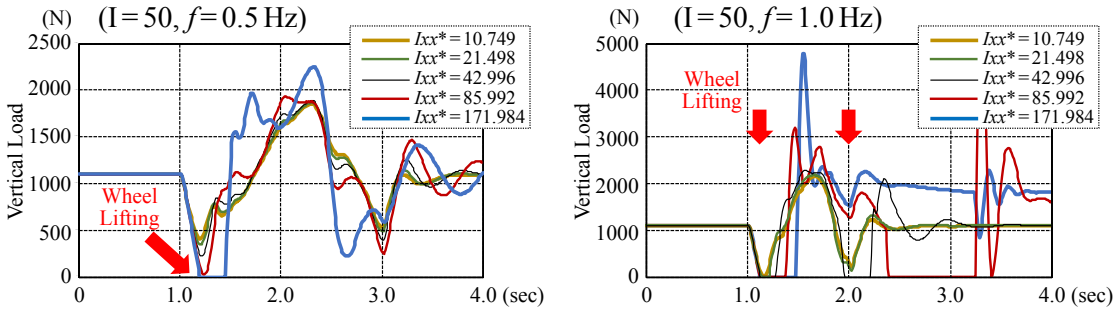

Figure 13. Influence of roll inertia moment to vertical load of front left wheel (I = 50)

3.2.2 Influence of pitch and yaw inertia moments

Influences of sprung pitch inertia moment *Iyy** and sprung yaw inertia moment *Izz** were examined as shown in Figures 14. However, no significant influences were observed on front inner wheel lifting phenomena. Therefore, we decided to concentrate to roll direction mechanism 1) been prospected on former section 3.1.

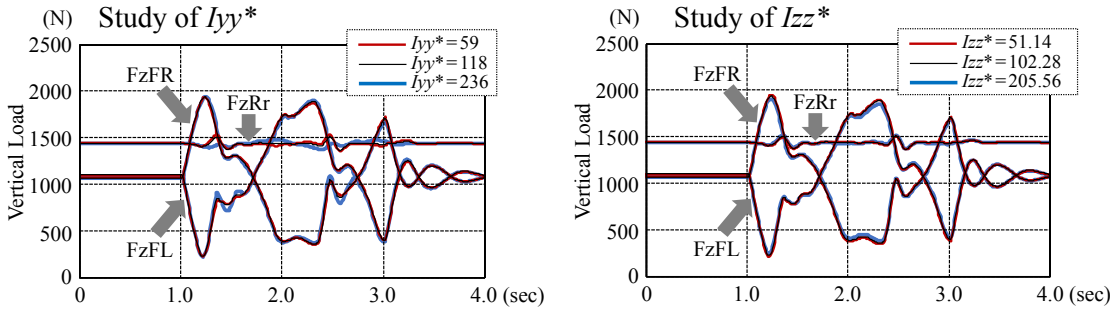

Figures 14. No significant influences were observed with pitch and yaw inertia moment (I = 50)

3.2.3 Roll resonance frequency *fφ* and influence of roll dynamics

PMVs have half total width (equivalently 1/4 roll inertia moment) and have half front tread (equivalently 1/4 front roll stiffness) compared with passenger cars. PMVs have no roll stiffness on rear wheel (equivalently 1/8 total roll stiffness). Thus, as shown in Equation (4), roll resonance frequency *fφ* is judged to be further low (equivalently $1/\sqrt{2}$).

$$f\varphi \propto \left(\frac{K\varphi}{Ixx}\right)^{1/2} \quad \cdot \cdot \cdot (4)$$

fφ ; Roll resonance frequency
Kφ ; Roll stiffness
Ixx ; Roll inertia moment

Therefore, we grasp roll resonance frequency $f\varphi$, experimentally at first. While driving straight at 36 km/h (10 m/sec), a roll pulse was input by a sharp steering pulse (± 30 deg, 8 Hz, one cycle of sinusoidal input) as shown in Figure 15. After pulse input, remained roll vibration was observed and its frequency was about 1.67 Hz. This roll resonance frequency $f\varphi$ is on suspension roll stiffness, not related to tilting mechanism.

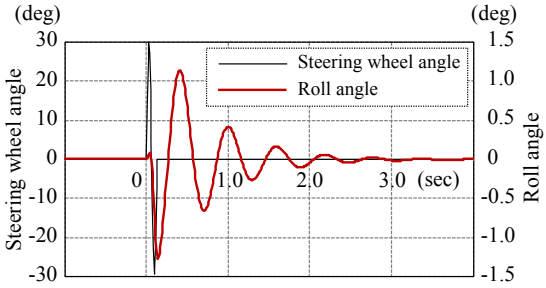

Figure 15. Roll resonance frequency is about 1.67 Hz (I = 100)

As shown in Figure 16, vehicle mass, spring/stabilizer-bar stiffness of suspension, damping force characteristics, and roll tracking control gains P, I, D were all doubled in order to get vehicle characteristics with equivalently same roll dynamics. Then, front inner wheel lifting phenomena showed almost same characteristics as reference vehicle. From this, it was confirmed that front inner wheel lifting phenomena are almost dominated by roll dynamics of PMVs.

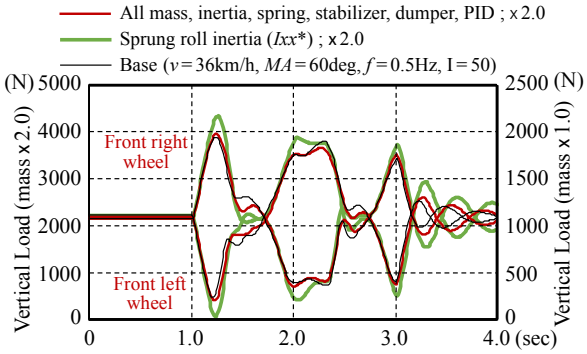

Figure 16. Equivalently same roll dynamics gives same wheel lifting phenomena

3.3 Summary of this section and setting specifications for further study

- Lateral displacement *LD* is proportional to steering angle *MA* and square of vehicle speed *v*, and inversely proportional to square of steering input frequency *f*.

- Increase of steering input frequency *f* itself is disadvantageous for front inner wheel lifting. Increase of input steering wheel angle *MA* to maintain lateral displacement *LD* on increase of steering input frequency *f*, causes further severe condition of front inner wheel lifting.

- Increase of vehicle speed *v* requires quicker steering input frequency *f*, which is disadvantageous for front inner wheel lifting.

- Inner wheel lifting phenomenon is only that vehicle roll is unavailable to follow target roll angle *TRA* due to sprung roll inertia moment *Ixx** and is almost dominated by roll dynamics of PMVs. Smaller *Ixx** and larger $K\varphi$, i.e. higher roll resonance frequency $f\varphi$ improves front inner wheel lifting phenomena.

- Unstable roll phenomena without intentional steering input related to front inner wheel lifting phenomena is suppressed by decrease of I gain of PID tracking control to active roll angle. In order to study realistic roll inertia moment *Ixx** and roll stiffness $K\varphi$, PID control parameters in further study are set as Equation (5).

$$P = 4000\,, \quad I = 50\,, \quad D = 0 \qquad \cdot\cdot\cdot \quad (5)$$

4 CAPABILITY ON OBSTACLE AVOIDANCE

4.1 Comparison front wheel steering (FWS) and rear wheel steering (RWS)

Recently, Toyota Motor Corporation had introduced active tilting type PMV concept vehicle with RWS, considering package advantage. However, RWS system is not general in the market. Comparison FWS and RWS in obstacle avoidance point of view is necessary. [5]

4.1.1 Understanding of vehicle posture on avoidance behaviour

Although there is no difference between FWS and RWS in Equation (6) that describes vehicle condition on steady circle, RWS vehicles show clearly inward posture (rear end pushed out) as shown in Figure 17.
Image of vehicle posture on left direction avoidance is shown on Figure 18. Rear vehicle end moves to right at first in RWS, and this makes delay of lateral displacement *LD* of RWS vehicles.

$$\rho = \left(1 - \frac{m}{2l^2}\frac{l_f K_f \quad l_r K_r}{K_f K_r} v^2\right)\frac{l}{\delta} \qquad \cdot\cdot\cdot (6)$$

ρ ; Turning Radius
m ; Vehicle Mass
l ; Wheel Base
l_f ; Front Wheel Base
K_f; Front Cornering Power
l_r ; Rear Wheel Base
K_r; Rear Cornering Power
v ; Velocity
δ ; Tire Steer Angle

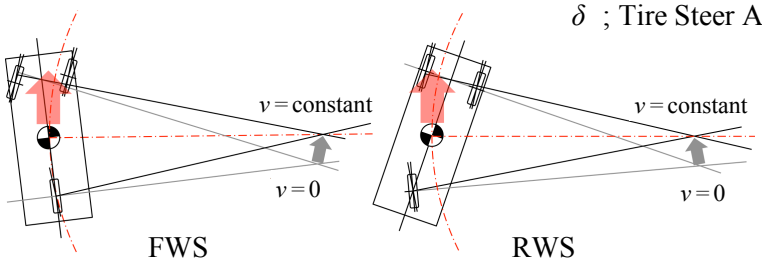

Figure 17. Vehicle postures on steady state cornering

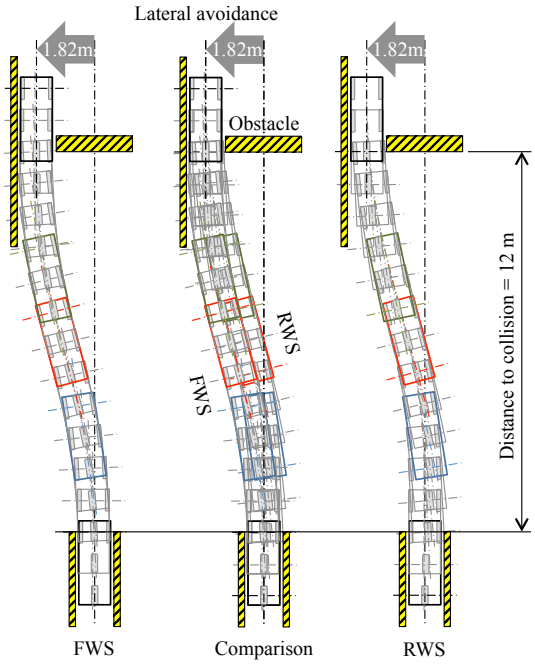

Figure 18. Tracks image of FWS and RWS to avoid obstacle

4.1.2 Open loop simulation

First, open loop simulations were operated by steering angle input as shown in left of Figure 19. Vehicle speed was fixed at 36 km/h and lateral displacement was 1.82 m achieved with sinusoidal steering input. Delay of lateral displacement *LD* in RWS assumed in former section is also shown in comparison using dynamic simulation tool as apparent from right of Figure 19. It is approximately 2 m delay in longitudinal distance under this condition.

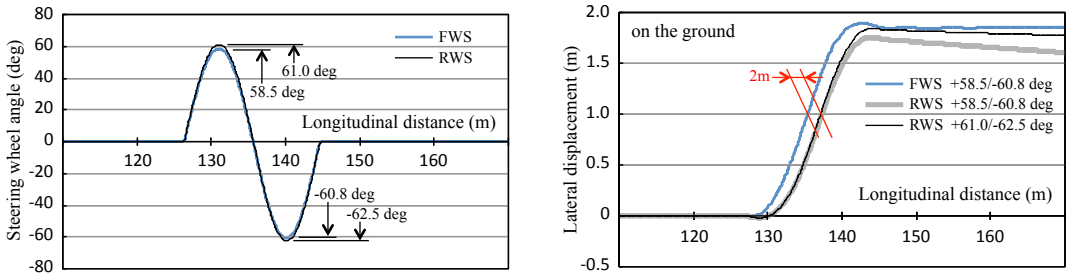

Figure 19. Steering wheel angle and lateral displacement on open loop simulation

4.1.3 Closed loop simulation

Pylon-controlled single lane change course was set for closed loop simulation as shown in Figure 20. Maximum steering angle, maximum steering speed, and maximum steering acceleration are all sufficiently large for avoidance operation.

In closed loop, driver recognizes given lane change course in advance. Therefore, it makes easier to pass by steering a little to opposite side before starting avoidance as shown in left of Figure 21. However, it is impossible to avoid oncoming obstacles by this way in real world.

As shown in Figure 21, in case of FWS, rise of steering angle after start of avoidance is a little gentle, and steering angle is considerably smaller and longer in latter half of avoidance, than in open loop. In case of RWS, large steering angle is required to recover delay of open loop avoidance. It is about 1.6 times larger angle in first half of avoidance and about twice angle in second half. Overshoot at end of avoidance is also noticeable, indicating difficulty of avoidance operation in RWS.

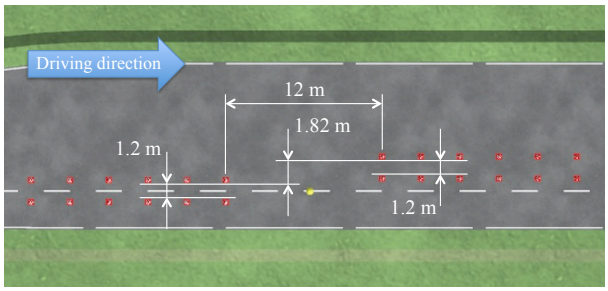

Figure 20. Single lane change course as obstacle avoidance

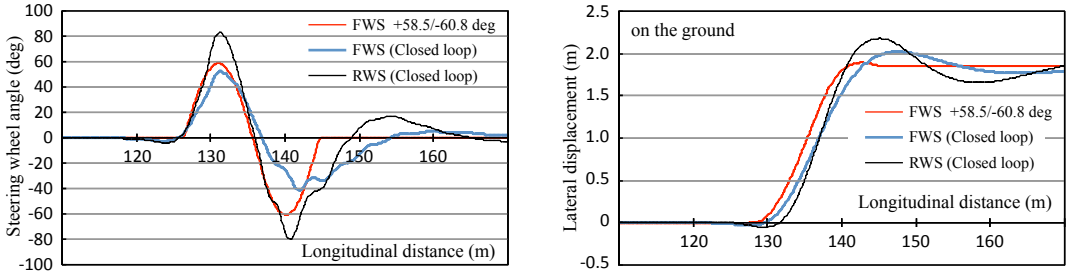

Figure 21. Steering wheel angle and lateral displacement

4.1.4 Judgment of FWS and RWS on implementation

Rear end of RWS vehicle is pushed out at first timing of avoidance, and this makes delay of lateral displacement. Superiority of FWS to RWS in obstacle avoidance performance was shown.

4.2 Comparison with passenger cars and motorcycles

Obstacle avoidance capabilities of motorcycles which are accepted in market are generally lower than those of passenger cars. When considering social acceptability of completely new PMVs with tilting mechanism, it is reasonable to compare them with those with market experience [6].

4.2.1 Vehicle models of passenger cars and motorcycles

CarMaker of IPG Automotive GmbH of Germany was used also as passenger car simulation tool, and accompanying general passenger car model was used as a vehicle model. For motorcycle, we used BikeSim from Mechanical Simulation, USA. Table 3 shows basic specifications of these vehicles.

Table 3. Specifications of Passenger car and Motorcycle

Passenger Car			Motorcycle		
item	unit	value	item	unit	value
Total length	m	4.15	Total length	m	2.14
Total width	m	1.70	Total width	m	0.637
Total height	m	1.60	Total height	m	1.318
Wheel base	m	3.185	Wheel base	m	1.576
Front tread	m	1.508	Front mass distribution	kg	122.77
Rear tread	m	1.494	Rear mass distribution	kg	75.48
Total mass	kg	1463	Total mass	kg	198.25
Gravity center height	m	0.58	Gravity center height	m	0.35

4.2.2 Driving course

Vehicle models drive in to single lane change course from approach section. Course severity was set as maximum passing speed would be normal driving speed. Three levels, 1.5 m, 2.0 m and 2.5 m, of lateral displacement in 10 m transition section were set by parameter study in advance as shown in Figure 22. Situation is that vehicles run right end of lane and obstacle is at right end of lane. This means severer situation for narrower vehicles, PMVs and motorcycles.

Generally, lane width is set with a certain margin in vehicle width. Therefore, course widths are not same between PMV and motorcycle, and passenger car. However, lateral displacement levels are same and capabilities of obstacle avoidance were judged on maximum passing speeds.

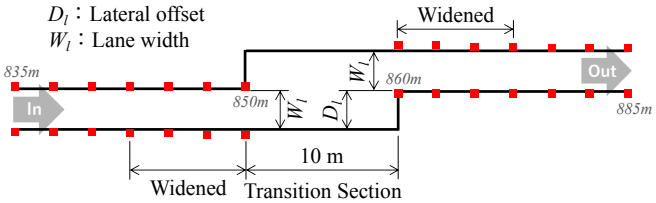

PMV, Motorcycle : W_l=1.5m D_l=1.5m, 2.0m, 2.5m
Passenger Car : W_l=2.32m D_l=1.5m, 2.0m, 2.5m

Figure 22. Three levels of severity on driving course were set by parameter study

4.2.3 Passing speed comparison and understanding social acceptability

In case of CarMaker, longitudinal speed is controlled consistently and automatically, but lateral control is switched from straight running model to automatic steering control model just before transition section. Straight running model runs middle of lane, but automatic driving model takes advantageous course (feint motion) as far as possible even if a narrow course width is set.

For this reason, after entering single lane change course, model is switched from straight running model to automatic driving model. Switching timing was set as early not to miss inner pylon and as late not to take advantageous course. Driver parameter and maneuver are shown in Table 4.

Table 4. Driver maneuvers were set to avoid feint motions

Driver		
item	unit	value
Corner Cutting Coefficient		0.1
Max. Long. Acceleration	m/s^2	3.0
Max. Long. Deceleration	m/s^2	-4.0
Max. Lat. Acceleration	m/s^2	20
PylonShiftFdCoef		0.15

Maneuver		
item		Model
Longitudinal Dynamics		IPGDriver
Lateral Dynamics	< 841.5m	Follow Course
(D_l=1.5m)	> 841.5m	IPGDriver
Lateral Dynamics	< 843m	Follow Course
(D_l=2.0m)	> 843m	IPGDriver
Lateral Dynamics	< 844m	Follow Course
(D_l=2.5m)	> 844m	IPGDriver

In PMVs and passenger cars, vehicle speed is automatically reduced when entering speed is quicker than passable speed. Therefore, in general, entrance speed (avoidance speed) to transition section and exit speed from transition section are different. In this study, entrance speed to transition section was used as passing speed. In case of PMV, only once front inner wheel lifting was accepted, but repeated liftings were judged to be failed.

In case of BikeSim, autonomous maximum speed driving in given course is not possible. Target trajectory was given to rider model to drive similar course to PMV. Preview time was set according to model switching distance in PMV and riding manner was adjusted by behavior gain of tilting. Speed was gradually increased and it was judged from actual trajectory whether it was successful or not. Target trajectory was adjusted to get maximum passing speed in necessity.

Comparison of maximum avoidable speeds is shown in Figure 23. As is generally understood, it was confirmed that there is large difference between passenger cars and motorcycles. Capability of obstacle avoidance on PMVs is not only clearly superior to motorcycles, but also at equal to or higher than passenger cars. Therefore, we may understand PMVs have sufficiently social acceptability in terms of capability of obstacle avoidance.

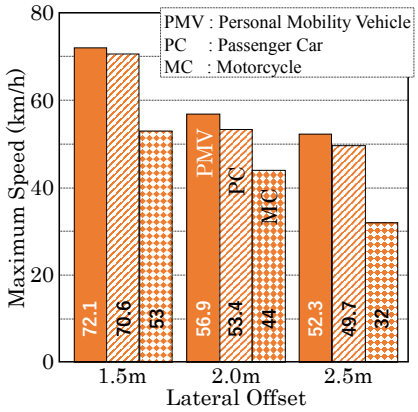

Figure 23. Comparison of capabilities on obstacle avoidance

4.2.4 Mechanism of superiority of PMV

As shown in Figure 24, on dynamics of passenger cars, centrifugal force acting on gravity center height (G.C.H.) and supporting force on ground height make roll moment, and lateral transfer of vertical load make opposite direction roll moment. These two moments are balanced each other and balance angle is expressed by Equation (7).

In motorcycles, there are no lateral transfer of vertical load. Roll moment due to centrifugal force acting on G.C.H. is balanced by roll moment due to couple of vertical forces. Moment arm length in lateral direction is caused by actual vehicle roll angle. This is balance angle of single-track vehicles such as bicycles and motorcycles. This is expressed by Equation (8).

$$\tan\varphi_e = \tan\varphi_t = d_t / \text{G.C.H.} \quad \cdots (7)$$

φ_e : Equivariant roll angle
d_t : Moment arm length on lateral transfer of load
G.C.H. : Gravity Center Hight

$$\tan\varphi_e = \tan\varphi_a = d_a / \text{G.C.H.} \quad \cdots (8)$$

φ_a : Actual roll angle
d_a : Moment arm length on actual roll

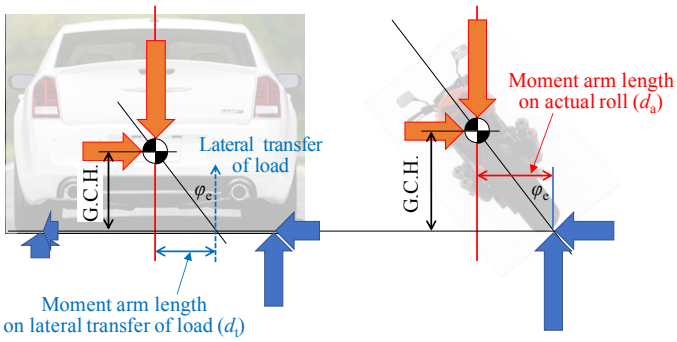

Figure 24. Roll moment balance on Car and Motorcycle

In PMVs with active tilting mechanism, couple of strokes on both wheels are given to get roll angle. This is equivalent to positively generating lateral transfer of vertical load. After roll angle is obtained as equivariantly same as motorcycles, vertical loads of both wheels settle equally as a result. But while response of roll angle is delayed, lateral transfer of vertical load occurs between both wheels like passenger cars.

As shown in Figure 25, roll moment due to lateral transfer of vertical load is same as that of passenger cars, and roll moment due to actual roll angle of vehicle body is same as that of motorcycles. This is expressed by Equation (9). In dynamics of passenger cars, lateral force and lateral acceleration on front body occur without any delay due to front tires slip angle by steering angle input. However, since roll inertia moment balances dynamically with roll moment due to lateral acceleration, there is a slight delay in lateral transfer of vertical loads. In motorcycles, lateral acceleration can only be obtained when inward roll occurs in vehicle body. This is a factor that causes a large delay in lateral acceleration of motorcycles (slow avoidance motion), while delay in lateral acceleration of passenger car is not conspicuous in avoiding obstacles.

$$\begin{aligned}\tan\varphi_e &= \tan\varphi_a + \tan\varphi_t \\ &= (d_a + d_t) / \text{G.C.H.} \quad \cdots (9)\end{aligned}$$

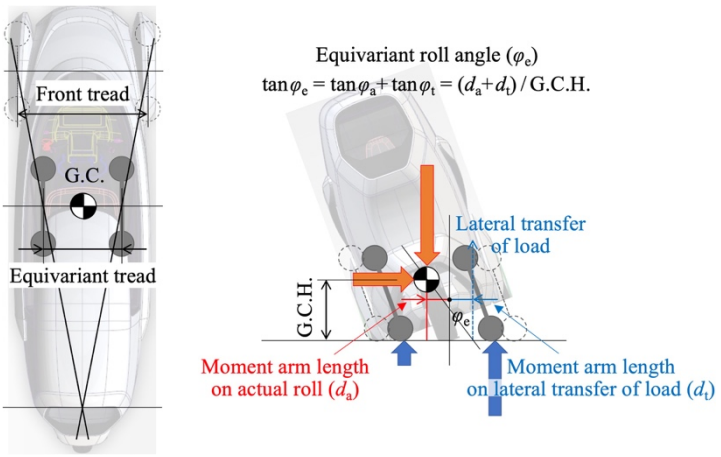

Figure 25. Roll moment balance on PMV with active tilting mechanism

In case of PMVs with actively applied roll angle, as shown in left of Figure 26, lateral transfer of vertical loads occurs with no delay according to steering angle input. In comparison with motorcycle, it is equivalent to giving virtual additional roll angle, during delay of actual roll angle by tracking control and by roll inertia moment. These two roll angles are shown in right of Figure 26. Actual roll angle reaches its peak near center of transition section, but additional virtual roll angle already balances with lateral acceleration in opposite direction at same timing.

As shown in Figure 27, sum of actual roll angle of vehicle body and virtual roll angle of PMVs corresponds equivalently to inward roll angle of motorcycles. Since this equivalent roll angle balances with lateral acceleration, PMVs are able to provide lateral acceleration without response delay, as same as passenger cars.

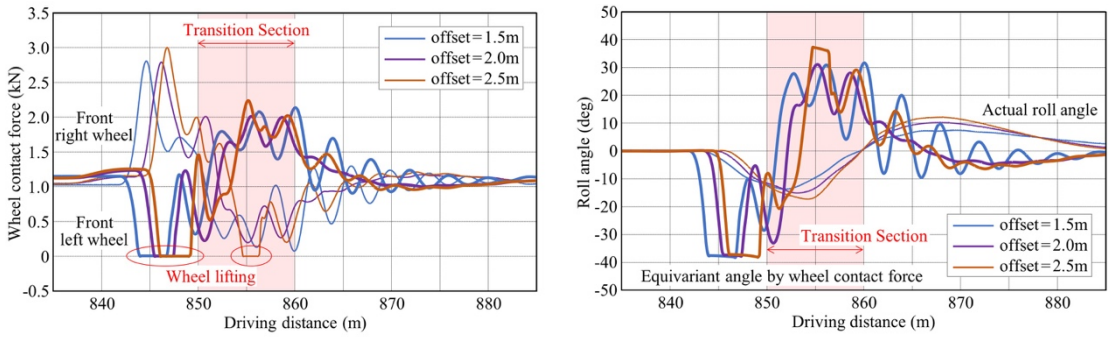

Figure 26. Lateral load transference and equivariant roll angle on load transference

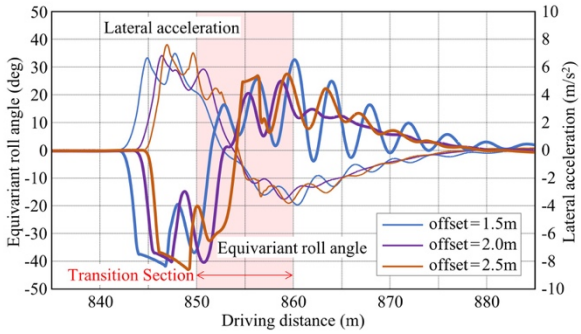

Figure 27. Balance of lateral acceleration and equivariant roll angle

4.3 Summary of this section

In comparison capabilities of FWS and RWS on obstacle avoidance, it was understood that RWS has behavior of rear end pushed out at first timing and makes delay of lateral displacement. By dynamic simulation, it was shown especially difficulty for driver to steer to cover delay and avoid obstacle in RWS. Therefore, it can be judged that FWS is superior than RWS in obstacle avoidance performance.

PMVs with active tilting mechanism have obstacle avoidance ability equal to or higher than that of passenger cars, because they have much smaller roll inertia moment than passenger cars and responsiveness equivalent to passenger cars. Thus, sufficient social acceptance from capability of obstacle avoidance of PMVs with active tilting mechanism could be confirmed also from their dynamic mechanism.

5 ENERGY CONSUMPTION ON ACTIVE TILTING SYSTEM

Although PMVs with passive tilting mechanism have negative point of lack of self-standing ability in stopping and in very low speed as same as motorcycles, PMVs with active tilting mechanism have not such concern. On the other hand, there is a concern about contradiction

with efficiency improvement inherent in PMVs, since energy consumption is inevitably unavoidable in active tilting mechanism [7].

5.1 Mechanism of energy balance

5.1.1 Energy consumption in active tilting mechanism

Although, it is originally necessary to describe twist energy of stabilizer bar to sprung body independently of bounce strokes of front both wheels, consumed twist energy can be expressed by product of difference of vertical loads from mean value and difference of bounce strokes from mean value, as shown in Equations (10), (11) and Figure 28.

Energy efficiencies in actuating and recovering should be considered. In this study, actuating efficiency was set to 0.5 and recovering efficiency was set to 0.1 as an electrical general value.

$$\Delta E = Fz_L \times \Delta Sz_L + Fz_R \times \Delta Sz_R \quad \cdots (10)$$

IF $\Delta E > 0$, $\Delta E^* = \Delta E \times 2$

(Actuator Energy Efficiency rate = 0.5)

IF $\Delta E < 0$, $\Delta E^* = \Delta E \times 0.1$

(Recovery Energy Efficiency rate = 0.1)

$$E = \Sigma \Delta E^* \quad E \text{ ; Energy} \quad \cdots (11)$$

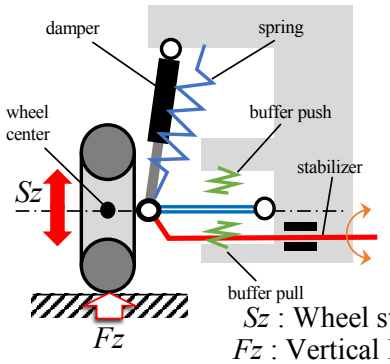

Figure 28. Energy consumption mechanism

5.1.2 Energy consumption by cornering drag in case of no tilting

Generally, centripetal forces for vehicles are given as lateral force (SF) by tire slip angle (SA) when vehicles turn. Useful cornering force (Y) for turning is represented as $SF \times \cos(SA)$. Orthogonal $SF \times \sin(SA)$ is cornering drag component, and energy is consumed wastefully.

Although vertical load of each tire is always changing, for simplicity, static load is substituted and tire Cornering power (K) is defined at this load as shown in Figure 29. Y is obtained from dynamic simulation and SA is obtained as dividing Y by K.

Total consumed energy rate caused by cornering drag is represented by product of cornering drag component and longitudinal distance of vehicle as shown in Equation (12). Then accumulated consumed energy is sum of consumed energy rate as shown in Equation (13).

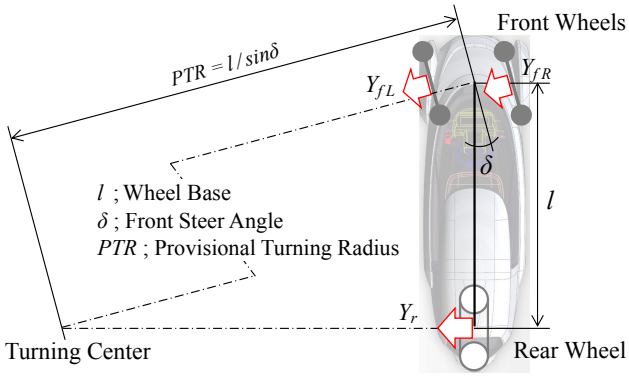

Figure 29. Energy consumption caused by cornering drag

$$\Delta E = Y_{fL} \times sin(Y_{fL}/K_{fL}) \times v \times \Delta t + Y_{fR} \times sin(Y_{fR}/K_{fR}) \times v \times \Delta t + Y_r \times sin(Y_r/K_r) \times v \times \Delta t \quad \cdots (12)$$

E ; Energy v ; Vehicle Velocity
Y ; Cornering Force t ; Time
K ; Cornering Power

$$E = \Sigma \Delta E \qquad \cdots (13)$$

5.2 Energy consumption in typical driving modes

Although there are various explanations for principle of side force generation due to camber angle, it is general that cornering drag component of side force by camber angle is not considered, because it has no slip angle.

In this section, under assumption that there is no cornering drag component of lateral force by camber angle, energy consumption for active roll angle is compared with energy saving by using camber angle. Then we consider social acceptability of PMVs with active inward tilting mechanism.

5.2.1 Energy consumption on steady circle

In PMVs with inward tilting like motorcycles, during turning on steady circle, roll moment due to centrifugal force is canceled by roll angle and no additional roll moment is necessary. In other words, energy consumption due to cornering drag can continue to be avoided without energy consumption for tilting.

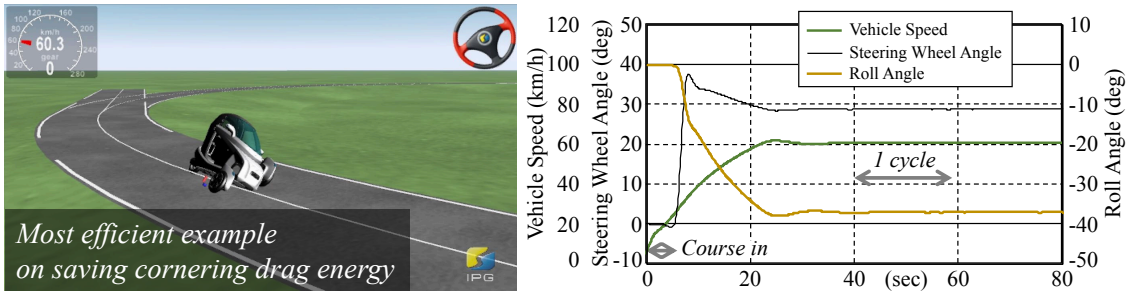

Figure 30. Driving on steady circle

Energy consumption due to tilting and cornering drag of PMVs while entering to circle course, 50 m turning radius, from straight course are shown. It starts on straight course, accelerates while entering to circle course and reaches steady speed of 60 km/h as shown in Figure 30. Tilting energy is consumed only for a short time, therefore accumulated energy consumption for tilting may be considered substantially zero as shown in left of Figure 31. On the other hand, cornering drag energy is saved continuously on circle course as shown in right of Figure 31.

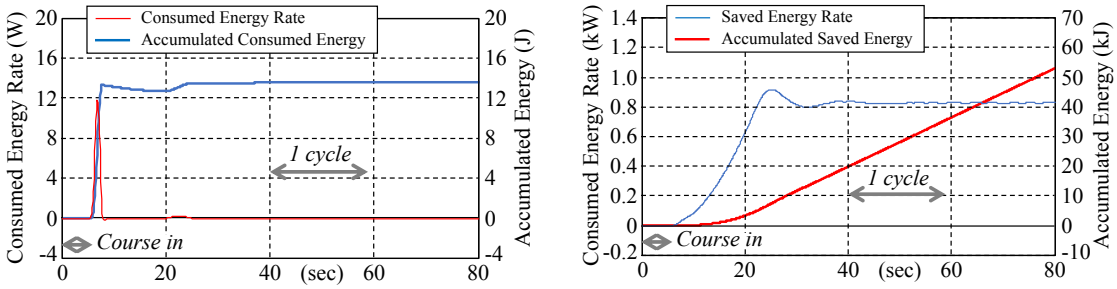

Figure 31. Consumed and saved energy on steady circle

5.2.2 Energy consumption in slalom

Contrary to steady circle, pylon slalom with repeated tilting is typical example of extremely consuming energy for tilting. We set slalom course with 10 pylons at 18 m interval as shown in Figure 32. Vehicle reaches 60 km/h before slalom section and passes through slalom section with constant speed.

IPGDriver prepares "corner cutting coefficient (ccc)" as one of model parameters of driver characteristics in virtual driving. ccc = 0 means driver runs middle of given course, and ccc = 1.0 means driver runs fully in-cut course. In other words, ccc = 1.0 is set to follow easiest course. Under this condition, with ccc = 0.4, driver could not pass given course because of overturning. Therefore, this course setting may be considered to be almost at limit condition.

Although, three levels of ccc were compared, which are ccc = 0.5, 0.7 and 0.9 as shown in Figure 33, no major difference was found in steering wheel angles as input and lateral vehicle accelerations as output. Therefore, we decided to proceed this study of energy balance at ccc = 0.7, which is considered to be a general driver characteristic.

In slalom, large amount of energy is consumed to give quick change in roll angle as shown in left of Figure 34. During this time, although energy saving caused by avoidance of cornering drag also occurs significantly as shown in right of Figure 34, this cannot offset energy consumption for tilting.

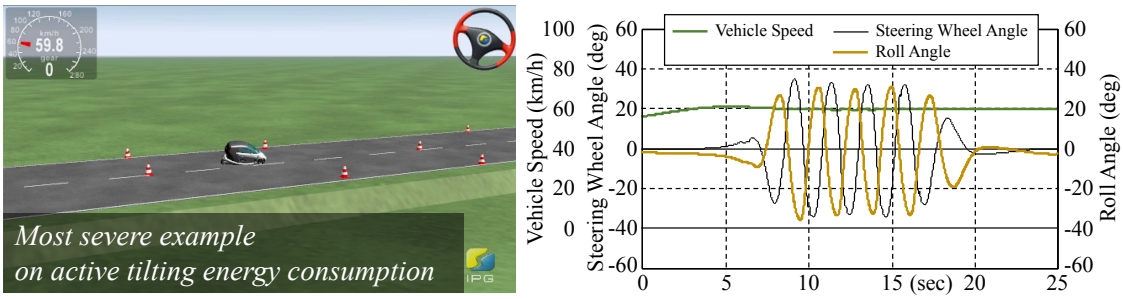

Figure 32. Driving on slalom course

ccc ; cornering cutting coefficient (Driver characteristics)
ccc = 0.0 ; No in-cut driving, 0.4 ; Overturning, 1.0 ; Maximum in-cut driving

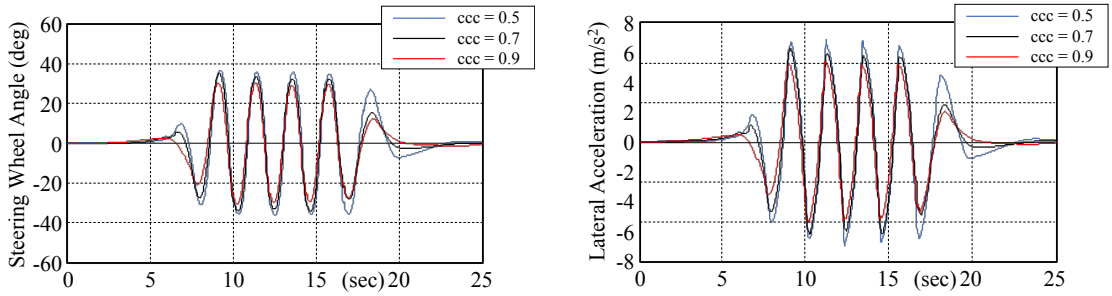

Figure 33. Influence of driver parameter is not significant

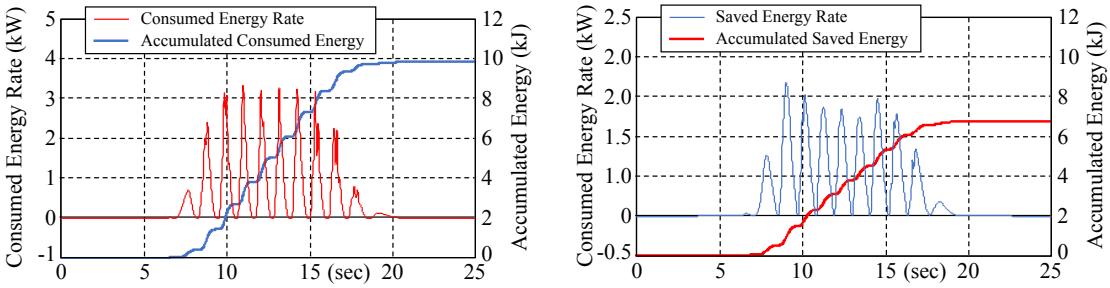

Figure 34. Consumed and saved energy on slalom course (ccc = 0.7)

5.3 Energy consumption in real world condition

Driving modes for homologation of fuel consumption are basically on straight course in all

countries, and do not assume steering wheel operation or lateral acceleration of vehicle. However, German "auto motor und sport (AMS)" magazine prepares its own evaluation course, which is round route of public road in South Germany.

5.3.1 Typical European evaluation course (AMS)

AMS evaluation course with total length of 92.5 km and elevation difference of 290 m is shown in Figure 35. It takes about 5,000 seconds to drive this PMV. Maximum speed is determined from speed regulation and limit of vehicle's performance. There are many stop intersections on this course. Steering wheel angle is particularly large when vehicle stops, starts and turns at these intersections.

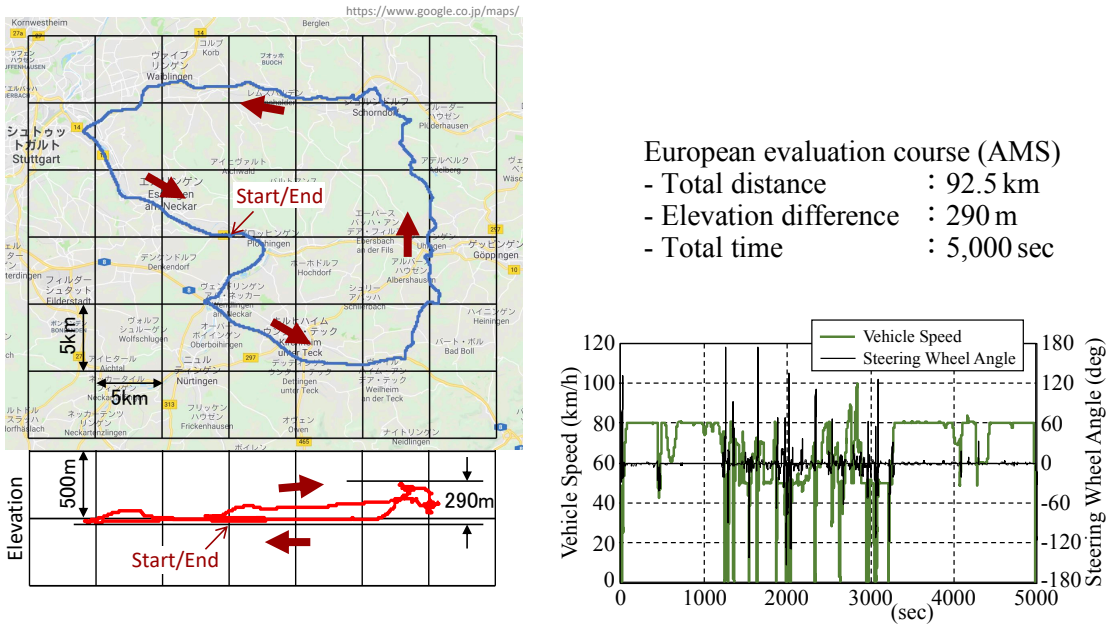

Figure 35. AMS evaluation course as typical European driving route

5.3.2 Energy consumption in AMS magazine evaluation course

As shown in left of Figure 36, energy consumption rate has sharp peaks at intersections and at tight corners, and accumulated consumed energy is less than 6 kJ in 5,000 seconds. This amount is fairly small.

As shown in right of Figure 36, energy saving cause by avoidance of cornering drag occurs much more frequently than energy consumption for tilting. This means that steering wheel holding time on cornering sections is much longer than steering input and return.

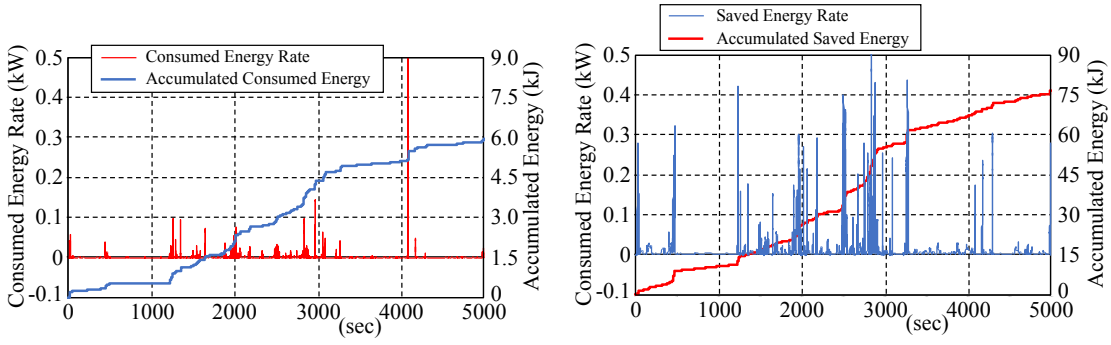

Figure 36. Consumed and saved energy on AMS evaluation course

There is difference in both energy rates, and larger difference in accumulated energy amounts. Accumulated energy saving against cornering drag reaches 76 kJ in 5,000 seconds.

As shown in Figure 37, there is about 13 times difference between two accumulated energies, and it shows no need to worry about energy consumption on active tilting mechanism. High precision in simulation model is not required at all for this definite result.

As shown in Table 2, total mass of vehicle including one passenger of this PMV is about 370 kg, and total vertical load is about 3,600 N. Assuming tire rolling resistance coefficient (RRC) is approximately 80×10^{-4}, tire rolling resistance is approximately 29 N. Energy of 2,700 kJ is consumed on 92.5 km course with this rolling resistance.

This energy, 2,700 kJ, is about 36 times of energy consumption by cornering drag, and 450 times of energy consumption on tilting mechanism as shown in Figure 37. Energy consumption on driving PMVs is overwhelmingly dominated by tire rolling resistance if acceleration/deceleration and air drag are not considered.

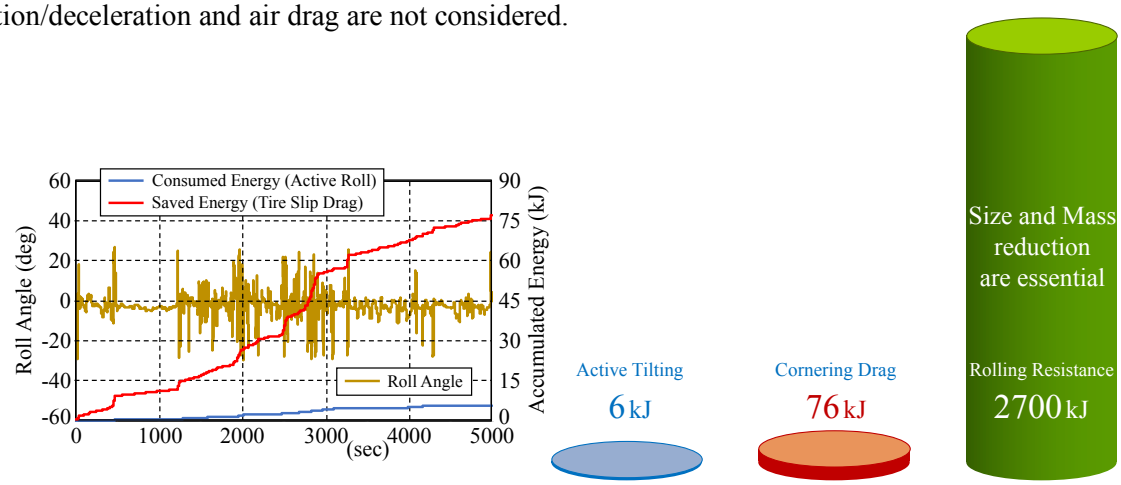

Figure 37. Energy balance on AMS course and comparison with rolling resistance energy

5.4 Social acceptance from viewpoint of energy consumption

Energy consumption for tilting is only about 1/13 of saving effect of cornering drag, then total efficiency of PMVs with inward tilting mechanism is better than without tilting mechanism. Additionally, smaller and lighter PMVs are significantly more efficient than general cars as shown in Figure 38. These benefits of PMVs with active inward tilting mechanism shows sufficient social acceptability.

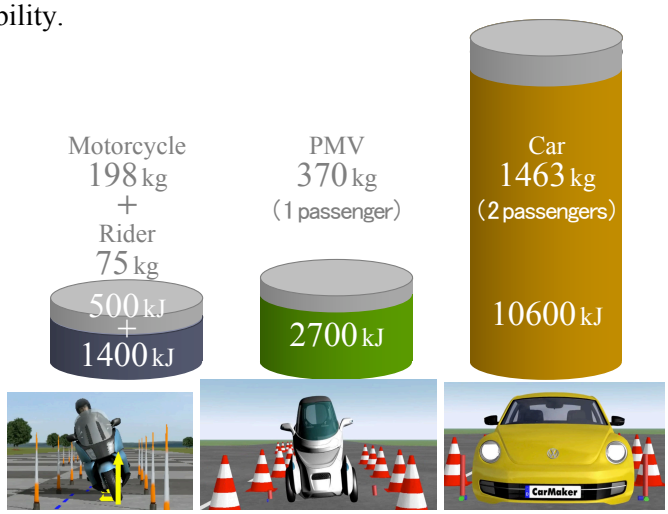

Figure 38. Comparison with energy consumption of general vehicles on rolling resistance

6 CONCLUSIONS

PMVs with active inward tilting mechanism with three wheels, double front wheels + single rear wheel and front steering + rear traction, are studied on front inner wheel lifting phenomena, on capability of obstacle avoidance and on energy balance of active tilting mechanism.

From following results, it was shown that PMVs with active inward tilting mechanism have sufficient social acceptability.

- Front inner wheel lifting phenomenon is only that vehicle roll is unavailable to follow target roll angle *TRA* due to sprung roll inertia moment *Ixx**. Smaller *Ixx** and larger $K\varphi$ improve front inner wheel lifting phenomena.

- It is possible to suppress unstable roll phenomena without intentional steering input related to front inner wheel lifting phenomena by decreasing of I gain of roll tracking control (PID).

- PMVs with active tilting mechanism have both advantages of vehicle dynamics. One is lateral transfer of vertical loads on front both wheels as same as general cars, and the other is inward tilting on turning as same as motorcycles.

- PMVs with active tilting mechanism have obstacle avoidance ability equal to or higher than that of passenger cars, because they have much smaller roll inertia moment than passenger cars and responsiveness equivalent to passenger cars.

- Energy consumption for active tilting mechanism is much smaller than energy saving by avoiding cornering drag by using camber angle. It shows no need to worry about energy consumption on active tilting mechanism.

- From general energy efficiency points of view, smaller and lighter PMVs are significantly more efficient than general cars, because rolling resistance caused by vehicle mass and tire rolling resistance coefficient, is major resistance of vehicles.

REFERENCES

[1] T. Kaneko, I. Kageyama, T. Haraguchi, Y. Kuriyagawa, “A Study on the Harmonization of a Personal Mobility Vehicle with a Lean Mechanism in Road Traffic (First Report)”, *Proceedings of JSAE Annual Congress (Spring)*, 2016, pp. 1350-1354.

[2] T. Haraguchi, “Are PMVs with inward tilting mechanism like motorcycles accepted in future mobility society?”, *Forum text of JSAE Annual Congress (Spring)*, 2019.

[3] T. Haraguchi, I. Kageyama, T. Kaneko, “Inner Wheel Lifting Characteristics of Tilting Type Personal Mobility Vehicle by Sudden Steering Input”, *Transactions of the Society of Automotive Engineers of Japan, Inc., Vol.50, No.1,* 2019, pp. 96-101.

[4] T. Kaneko, I. Kageyama, T. Haraguchi, “A Study on Characteristics of the Vehicle Response by Abrupt Operation and an Improvement Method for Personal Mobility Vehicle with Leaning Mechanism”, *Transactions of the Society of Automotive Engineers of Japan, Inc., Vol.50, No.3,* 2019, pp. 796-801.

[5] T. Haraguchi, T. Kaneko, I. Kageyama, M. Kobayashi, T. Murayama, “Obstacle Avoidance Maneuver of Personal Mobility Vehicles with Lean Mechanism -Comparison between Front and Rear Wheel Steering-”, *Proceedings of JSAE Annual Congress (Spring)*, 2017, pp. 494-499.

[6] T. Haraguchi, T. Kaneko, I. Kageyama, “Study on Steering Response of Personal Mobility Vehicle (PMV) by Comparison of PMV with Passenger Cars and Motorcycles on the Obstacle Avoidance Performance”, *Proceedings of JSAE Annual Congress (Autumn)*, 2018.

[7] T. Haraguchi, T. Kaneko, I. Kageyama, “Market Acceptability Study on Energy Balance of Personal Mobility Vehicle (PMV) with Active Tilting Mechanism”, *Proceedings of JSAE Annual Congress (Spring)*, 2019.